Paramagnetic Resonance Hyperfine Structure of Tetravalent Pa^{231} in Cs_2ZrCl_6†

J. D. Axe
Department of Chemistry and Lawrence Radiation Laboratory, University of California, Berkeley, California

AND

H. J. Stapleton and C. D. Jeffries
Physics Department, University of California, Berkeley, California

(Received November 7, 1960)

Paramagnetic resonance absorption at 3-cm wavelengths is observed for tetravalent Pa^{231} in a single crystal of Cs_2ZrCl_6 at helium temperatures. The observed spectra correspond to the allowed transitions $(S_z, I_z \rightarrow S_z \pm 1, I_z)$ and the forbidden transitions $(S_z, I_z \rightarrow S_z \pm 1, I_z \mp 1)$ of a system described by the spin Hamiltonian, $H_s = g\beta \mathbf{H}\cdot\mathbf{S} + A\mathbf{I}\cdot\mathbf{S} - g_n'\beta\mathbf{H}\cdot\mathbf{I}$, with $S=\frac{1}{2}$, $I=\frac{3}{2}$, $|A|/h = 1578.6 \pm 1.4$ Mc/sec, $|g| = 1.1423 \pm 0.0014$, and $|g_n'| \approx 8\times10^{-4}$. The errors indicate a small deviation from isotropy. It is further observed that $g_n'/g < 0$, indicating that if g_n' is positive, as is strongly indicated by the nuclear shell model, then g is negative. An additional electron-nuclear double-resonance experiment is used to determine directly the nuclear magnetic moment $\mu(Pa^{231}) = 1.96$ nuclear magnetons. This value includes a correction of 9% due to perturbations of an excited state about 1900 cm^{-1} above the ground-state doublet of Pa^{4+} in its octahedral crystal field. A lower frequency double-resonance experiment is used to measure the weak hyperfine interaction of the Pa^{4+} ion with its Cs^{133} neighbors, of order $A''/h \approx 0.5$ Mc/sec.

I. INTRODUCTION

PROTACTINIUM probably has an electron configuration of radon plus $5f^2 6d^1 7s^2$. The tetravalent ion Pa^{4+} was expected to be paramagnetic, the magnetic electron being either $5f^1$ or $6d^1$. The observation of paramagnetic resonance absorption by Axe, Kyi, and Stapleton,[1] in the crystal $Cs_2(Zr,Pa)Cl_6$ established the existence of a stable Pa^{+4} ion in this matrix. The resonance spectrum is isotropic with a spectroscopic splitting factor $|g| \approx 1.14$ and displays a large hyperfine structure of Pa^{231}. The results favor an f^1 electron configuration. In the present paper, we report on additional work to determine the sign of g and describe an electron-nuclear double resonance experiment to determine directly the nuclear magnetic moment of Pa^{231}, and a similar experiment to measure the weak hyperfine interaction of Pa^{4+} with its Cs neighbors in the crystal lattice.

The theory of an f^1 electron in an octahedral crystal field is briefly reviewed in Sec. II, as well as the energy levels and transitions pertinent to paramagnetic resonance. Details of the chemical preparation of the crystals and a description of the paramagnetic resonance apparatus are in Sec. III. In Sec. IV are presented the results of magnetic resonance experiments and their interpretation using preliminary data from additional optical absorption measurements.[2]

II. THEORY

The Pa^{4+} ion, when substituted for Zr^{4+} in Cs_2ZrCl_6 (see Fig. 1), is at the center of an octahedron of Cl^- ions and the problem at hand is similar to that of Np^{6+} in UF_6 as treated earlier by Hutchison and Weinstock.[3] The theory of an f^1 configuration in a crystal field of octahedral symmetry has been considered in detail by Eisenstein and Pryce,[4] whose notation and results we use here.

It is convenient to consider a Hamiltonian in the form

$$H = H_0 + H_{\text{oct}} + \zeta \mathbf{s}\cdot\mathbf{l}, \tag{1}$$

where the first term corresponds to the spin-independent portion of the free-ion Hamiltonian, the second to the octahedral potential supplied by the crystal field, and the last to the spin-orbit interaction. The second and third terms are of the same order of magnitude in the present case. Neglecting electronic spin initially, H_0 leaves degenerate the seven orbital states which we may take to be in an $|l=3, l_z\rangle$ representation. Upon immersion in an electrostatic field of octahedral symmetry, the degeneracy of the configuration is partially lifted in a manner prescribed by the decomposition of the $l=3$ representation of the full rotation group into representations of the cubic point group Θ. In this case $l=3 \rightarrow \Gamma_2+\Gamma_4+\Gamma_5$ (using Bethe's notation) and the energy levels are shown schematically in Fig. 2(b). If we set $E(\Gamma_2)=0$, $E(\Gamma_5)=V$, and $E(\Gamma_4)=V'$, the quantities V and V' may be regarded as the parameters which characterize the action of an octahedral field upon f electron configurations (analogous to the parameter Dq used for d electron configurations in octahedral fields).

When the intrinsic spin of the electron is taken into account, the number of eigenstates is doubled and they must now be characterized as basis functions for the octahedral double group. Since the spin function trans-

† This work was supported in part by the U. S. Atomic Energy Commission and the Office of Naval Research.

[1] J. D. Axe, R. Kyi, and H. J. Stapleton, J. Chem. Phys. 32, 1261 (1960).

[2] The optical absorption experiments are described in detail by J. D. Axe, thesis, University of California, 1960, issued as Rept. UCRL-9293, Lawrence Radiation Laboratory, Berkeley, California.

[3] C. A. Hutchison, Jr., and B. Weinstock, J. Chem. Phys. 32, 56 (1960).

[4] J. C. Eisenstein and M. H. L. Pryce, Proc. Roy. Soc. (London) A255, 181 (1960).

forms according to the representation Γ_6, the new basis functions which result transform as $\Gamma_2\times\Gamma_6=\Gamma_7$, $\Gamma_4\times\Gamma_6=\Gamma_6+\Gamma_8$, and $\Gamma_5\times\Gamma_6=\Gamma_7+\Gamma_8$. Addition of the spin-orbit interaction further removes the degeneracy as shown in Fig. 2(c). The splittings shown, Fig. 2(d), are the preliminary results of infrared absorption measurements, to be reported in a later paper.

It should be remarked that we consider the effect of covalent bonding to be negligible in the system which we are considering and have set the parameters k and k' which Eisenstein and Pryce introduce to cope with these effects to unity. They find it unnecessary to invoke covalency in NpF_6, and we feel that these effects should be even less pronounced in the $PaCl_6^{=}$ complex because of the appreciably longer ligand distances involved.

The crystal structure of Cs_2ZrCl_6 is that of K_2PtCl_6, a portion of which is shown in Fig. 1. When a protactinium ion is placed in a Zr^{4+} site in this structure, we should expect the lowest lying orbital states (in the absence of spin-orbit coupling) to be those which most successfully avoid the negative charge density about the chloride ions lying on the axes of the octahedron. As a consequence of this we should expect $V'>V>0$, and if this is so it is not difficult to show that upon introduction of spin-orbit interaction a doubly degenerate Γ_7 state lies lowest regardless of the relative magnitudes of crystal field vs spin-orbit interaction (see, for example, the diagrams presented by Hutchison and Weinstock[3]). We shall therefore principally focus our attention on the magnetic properties of Γ_7 states, although as we shall see, certain second-order corrections to the nuclear

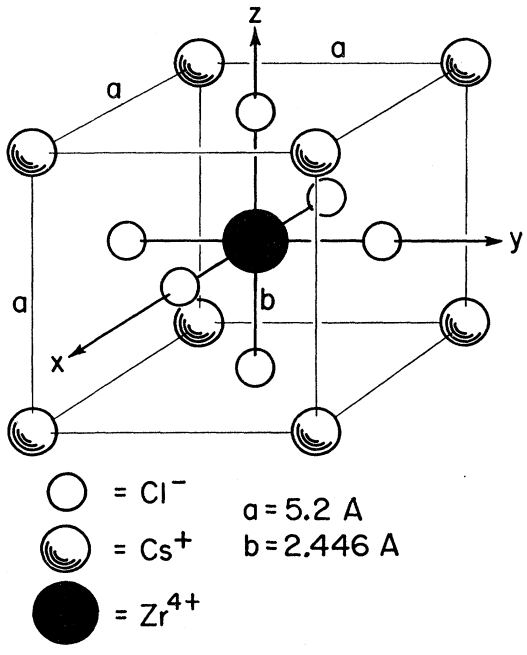

FIG. 1. Crystal structure of Cs_2ZrCl_6; alternate cubes have no central $ZrCl_6^{=}$ complex. The wave functions in Eq. (4) are in terms of the x, y, z axes shown.

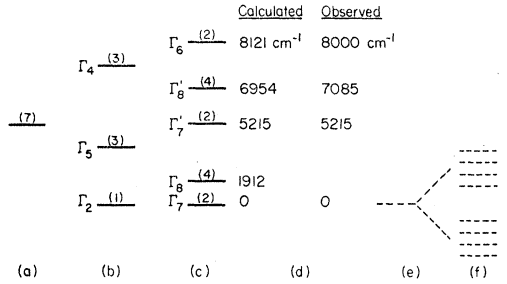

FIG. 2. Schematic energy level diagram of Pa^{4+} ion with various interactions: (a) free ion, no spin, 7-fold orbital degeneracy; (b) splittings into an orbital singlet and two triplets due to addition of crystal field of octahedral symmetry; (c) additional splitting due to spin-orbit coupling (total degeneracy shown in parenthesis); (d) splittings measured in infrared optical measurements compared to fitted values; (e) splitting of lowest doublet by magnetic field; (f) additional splitting due to hyperfine interaction with nuclear spin $I=\frac{3}{2}$.

moment will require some further consideration of the excited states of the system. Of course, at helium temperatures, essential for the observation of paramagnetic resonance, only the lowest doublet is populated.

The two degenerate lowest lying states, $|a\rangle$ and $|b\rangle$, will be linear combinations of the basis states $|A\rangle$, $|B\rangle$ and $|\bar{A}\rangle$, $|\bar{B}\rangle$:

$$\begin{aligned}|a\rangle&=\cos\theta|A\rangle-\sin\theta|B\rangle,\\ |b\rangle&=\cos\theta|\bar{A}\rangle-\sin\theta|\bar{B}\rangle,\end{aligned}\tag{2}$$

where

$$\begin{aligned}|A\rangle&=i|\beta\rangle, \quad |B\rangle=[|\epsilon_1\rangle+|\bar{\epsilon}_2\rangle+i|\bar{\epsilon}_3\rangle]/\sqrt{3},\\ |\bar{A}\rangle&=i|\bar{\beta}\rangle, \quad |\bar{B}\rangle=[-|\bar{\epsilon}_1\rangle+|\epsilon_2\rangle-i|\epsilon_3\rangle]/\sqrt{3}.\end{aligned}\tag{3}$$

Here β, $\epsilon_1\cdots$ represent the product of an orbital wave function and a spin-wave function, a bar, e.g., $\bar{\beta}$ indicating a $M_s=-\frac{1}{2}$ state, and the absence of a bar a $M_s=+\frac{1}{2}$ state. The orbital part is given explicitly by the Legendre polynomials of third degree:

$$\begin{aligned}\beta&\propto(105)^{\frac{1}{2}}xyz,\\ \epsilon_1&\propto(105)^{\frac{1}{2}}z(x^2-y^2)/2,\\ \epsilon_2&\propto(105)^{\frac{1}{2}}x(y^2-z^2)/2,\\ \epsilon_3&\propto(105)^{\frac{1}{2}}y(z^2-x^2)/2.\end{aligned}\tag{4}$$

The coordinate axes are the symmetry axes of the octahedron of Cl^- ions, Fig. 1. The mixing coefficient θ is determined by diagonalization of the Γ_7 matrix, which yields the equation:

$$\tan\theta=\{\tfrac{1}{2}-(V/\zeta)+[(V/\zeta)^2-(V/\zeta)+(7/2)^2]^{\frac{1}{2}}\}/2\sqrt{3}.\tag{5}$$

If a magnetic field H is applied, the Γ_7 doublet splits as in Fig. 2(e). It is straightforward to show that the first-order Zeeman effect within the Γ_7 manifold, can be written in the "spin Hamiltonian" formalism by replacing the operator $\beta(\mathbf{l}+2\mathbf{s})\cdot\mathbf{H}$ by $g\beta\mathbf{H}\cdot\mathbf{S}$ and the eigenvectors $|a\rangle$ and $|b\rangle$ by the angular momentum eigenvectors $|S=\frac{1}{2}, S_z=\frac{1}{2}\rangle$ and $|S=\frac{1}{2}, S_z=-\frac{1}{2}\rangle$, respectively. Similar replacements can be made for the magnetic hyperfine interaction, which gives additional

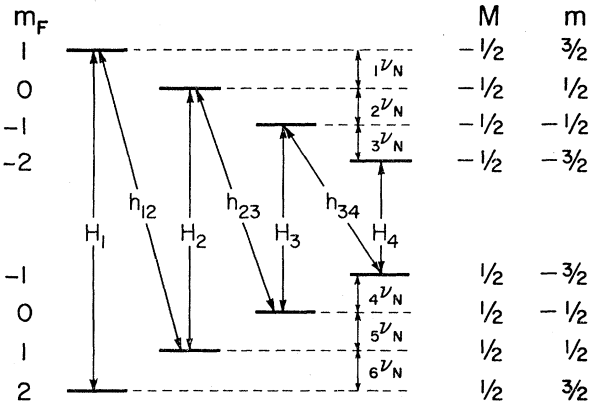

FIG. 3. Energy level diagram of ground state of tetravalent Pa^{231} in a large magnetic field. The transitions H_1, H_2, H_3, and H_4 correspond to the usual allowed transitions in paramagnetic resonance. The h_{12}, h_{23}, and h_{34} transitions are forbidden in zero order. The $_1\nu_n$, $_2\nu_n\cdots$ transitions are detected in double resonance experiments. In the ordering of the states it has been assumed that A and g in Eqs. (9) and (10) are negative.

splitting as in Fig. 2(f). An appropriate spin Hamiltonian for the Γ_7 level should thus be of the usual form,

$$H_s=g\beta\mathbf{H}\cdot\mathbf{S}+A\mathbf{I}\cdot\mathbf{S}-g_n'\beta\mathbf{H}\cdot\mathbf{I}, \tag{6}$$

with fictitious spin $S=\frac{1}{2}$, and

$$g=2\langle a|l_z+2s_z|a\rangle=2\cos^2\theta-4(1/3)^{\frac{1}{2}}\sin 2\theta, \tag{7}$$

$$A=4\beta^2g_n\langle r^{-3}\rangle\langle a|N_z|a\rangle=-\beta^2g_n\langle r^{-3}\rangle[8(1/3)^{\frac{1}{2}}\sin 2\theta], \tag{8}$$

where $\mathbf{N}=\mathbf{l}-\mathbf{s}+3(\mathbf{r}\cdot\mathbf{s})\mathbf{r}/r^2$, $g_n=\mu_n/I$, and μ_n is the nuclear magnetic moment in units of the Bohr magneton. For Pa^{231}, the nuclear spin $I=\frac{3}{2}$.[5] The small third term in Eq. (6) represents the nuclear Zeeman splitting, where we have used an effective nuclear g factor g_n', rather than the true nuclear g factor g_n because of possible corrections[6] due to the proximity of the Γ_8 state.

From an experimental viewpoint we consider that the magnitudes and the algebraic signs of g, g_n', and A are all unknown. For a free-electron spin, g would be positive for the sign convention used in Eq. (6). It should be noted that from nuclear shell-model theory,[7] there is good *a priori* evidence that g_n is positive for Pa^{231}, which should have a $p_{\frac{3}{2}}$ proton configuration with a magnetic moment roughly between the Schmidt and Dirac limits: $+3.87>\mu_n>+2.0$ nuclear magnetons.

In Fig. 3, the levels of Fig. 2(f) are shown to a larger scale; we have arbitrarily taken the sign choices $A<0$ and $g<0$. The magnetic states are labeled by their strong-field quantum numbers $\langle S_z\rangle=M$ and $\langle I_z\rangle=m$. For the fields used in our experiment the first term in Eq. (6) is dominant and the energy levels are approximately

$$W(M,m)\approx g\beta HM+AMm-g_n'\beta Hm. \tag{9}$$

We observe paramagnetic resonance absorption in the customary way by placing the crystal in a microwave cavity excited at the constant frequency $\nu\approx 10$ kMc/sec and varying the applied dc field H. Absorptions at the fields H_1, H_2, H_3, and H_4 in Fig. 3 correspond to the usual magnetic dipole transitions M, $m\rightarrow M\pm1$, m induced by that component of the oscillating microwave field which is perpendicular to H. In addition, absorptions at the fields h_{12}, h_{23}, and h_{34} correspond to the "forbidden" transitions M, $m\rightarrow M\pm1$, $m\mp1$. They are weaker by the factor $\approx(A/2g\beta H)^2$ and are induced by the parallel component of the oscillating field. Transitions of the type M, $m\rightarrow M$, $m\pm1$ can also be induced by applying a perpendicular oscillating field at the frequency $\nu_n\approx A/2h$. Such transitions can be detected very conveniently by the electron-nuclear double resonance (ENDOR) method of Feher,[8] wherein one observes the change in absorption at a frequency ν of one of the microwave resonance lines H_1, h_{12}, $H_2\cdots$ due to a population redistribution which occurs when the crystal is simultaneously irradiated at an ENDOR frequency ν_n. In principle there are six such frequencies $_1\nu_n$, $_2\nu_n\cdots$ for the system of Fig. 3, but their relative observability depends on unknown paramagnetic relaxation rates.

The unusually large value of $|A|$ and the precision required in our experiments necessitates the use of the Breit-Rabi expression for the exact energy levels of Eq. (6):

$$W(F=I\pm\tfrac{1}{2},m_f)=-A/4-g_n'\beta Hm_f \pm A(1+m_fx+x^2)^{\frac{1}{2}}\text{ ergs}, \tag{10}$$

where

$$x=[(g+g_n')\beta/2A]H, \tag{10a}$$

and

$$m_f=M+m=F,\quad F-1,\cdots -F.$$

It will be convenient to rewrite Eq. (10) in frequency units:

$$W/h=w(I\pm\tfrac{1}{2},m_f)=-\tfrac{1}{4}a+bHm_f \pm a[1+m_fCH+C^2H^2]^{\frac{1}{2}}\text{ cps}, \tag{11}$$

where

$$a=A/h\text{ cps},\quad b=-g_n'\beta/h\text{ cps oe}^{-1}, \tag{11a}$$

and

$$C\equiv(g+g_n')\beta/2A\text{ oe}^{-1}. \tag{11b}$$

III. SAMPLE PREPARATION AND PARAMAGNETIC RESONANCE APPARATUS

The compound Cs_2ZrCl_6 was prepared by refluxing stoichiometric amounts of anhydrous $ZrCl_4$ and CsCl for several hours in methanol saturated with HCl. The sparingly soluble product was obtained as a white precipitate, which was washed several times with fresh methanol and dried in a vacuum desiccator. The poly-

[5] H. Schuler and H. Gollnow, Naturwissenschaften **22**, 511 (1934).

[6] J. M. Baker and B. Bleaney, Proc. Roy. Soc. (London) **A245**, 156 (1958).

[7] M. G. Mayer and J. H. D. Jensen, *Elementary Theory of Nuclear Shell Structure* (John Wiley & Sons, Inc., New York, 1955), p. 58.

[8] G. Feher, Phys. Rev. **103**, 834 (1956).

crystalline material obtained in this manner was further purified by sublimation in vacuo at ~750°C in long (6-mm diameter) quartz tubes. The upper portions of the tubes containing the sublimate were sealed off (in vacuo) and single crystals were grown from a melt by slow passage through a crystal-growing furnace similar to that described by Gruen *et al.*[9] The crystals prepared in this way were generally highly transparent, free of microscopic flaws, and apparently were unaffected by atmospheric moisture.

Two methods of incorporation of tetravalent protactinium into the Cs_2ZrCl_6 matrix were used. The first method involved conversion of Pa_2O_5 into $PaCl_5$ by reaction with CCl_4, the reduction of $PaCl_5$ to $PaCl_4$ with H_2,[10] and regrowth of $PaCl_4-Cs_2ZrCl_6$ crystals from a mixed melt. A second method which avoided the manipulation of protactinium halides in vacuo consisted of reduction of Pa_2O_5 to PaO_2 with H_2,[10] and solution of the dioxide in molten Cs_2ZrCl_6 in subsequent passage through the crystal-growing furnace. We infer that $PaCl_4$ is formed by metathesis with zirconium chloride in the melt, since the PMR spectra obtained from crystals prepared by the two different methods were identical. The crystals grown by these methods had a mass of about one-half gram and contained from ~30 μg to 3 mg Pa^{231}. Spectrographic analysis of representative preparations of both pure and mixed crystals detected essentially equal small amounts (<0.1%) of common cationic impurities (Al, Ca, Mg, Fe, Na, and Si) in both samples.

A suitable crystal was encased in polystyrene and placed in the microwave cavity (Fig. 4) of a standard paramagnetic resonance spectrometer. The cavity is a brass cylinder, operating in the TE_{111} mode at ~9.3 kMc/sec and is immersed in and filled with liquid helium. A 12-in. electromagnet provides the dc field H, directed in a plane perpendicular to z'', Fig. 4. Relative values of H were measured by a motor driven flip-coil fluxmeter to an accuracy of ≈0.05%. The derivative of the paramagnetic resonance absorption was observed in the usual way by applying a small modulation field at 155 cps. A small piece of diphenyl-picryl-hydrazyl (DPH) was always placed on the sample holder to provide an absorption signal for the calibration of the fluxmeter.

An oscillating field at the ENDOR frequency ν_n (500 to 1200 Mc/sec) was applied to the sample by a one-turn wire loop about it (Fig. 4), so oriented that the coupling to the field of the cavity mode was negligible. The loop was driven by a General Radio Type 1021-P2 uhf signal generator equipped with a motor-driven frequency control. The frequency was measured every 5 Mc/sec or less, by beating with the harmonics of a standard quartz oscillator.

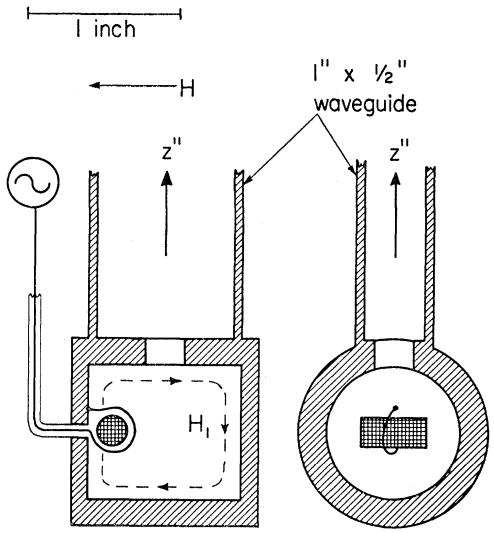

FIG. 4. Cavity of paramagnetic resonance apparatus, showing microwave magnetic field lines of TE_{111} mode ($\nu \approx 9.4$ kMc/sec), sample, and loop for applying fields at ENDOR frequency ν_n. The crystal may be rotated about the z'' direction.

IV. EXPERIMENTAL RESULTS AND INTERPRETATION

Figure 5 shows the paramagnetic resonance absorption derivative spectrum for Pa^{4+} in a single crystal of Cs_2ZrCl_6 at 1.6°K and $\nu = 9.168$ kMc/sec. No other resonance lines were seen for a field variation of $0 < H < 8.3$ kilo-oersteds, except for the DPH field marker line. The four strong lines labeled H_1, H_2, H_3, and H_4 correspond to the allowed transitions of Fig. 3 and confirm that the nuclear spin $I(Pa^{231}) = \frac{3}{2}$. The weaker lines labelled h_{12}, h_{23}, and h_{34} correspond to the forbidden transitions involving a simultaneous electron spin flip and nuclear spin flop. An identical spectrum was observed in several protactinium-containing crystals prepared in various ways, but was absent in "blank" crystals of Cs_2ZrCl_6. The lines are not observable at 77°K and have a temperature-independent width in the region $1.6°K < T < 4.2°K$ of about 20 oersteds peak to peak on the absorption derivative.

The crystal was rotated about the z'' axis of Fig. 4 and only a very small anisotropy in the spectrum was observed. The directions of the crystal axes were generally unknown, however, and we have not measured exactly the components of the g and the A tensors, but instead have simply established that they are isotropic to within one part in at least 300. Table I gives the measured values, within 1 oersted, of the allowed and forbidden lines for several angles. The field was calibrated in terms of the DPH resonance, using $g = 2.0038$.

We assume the Pa^{4+} spectrum is explicable in terms of the spin Hamiltonian, Eq. (6), and attempt to determine the three parameters A, g_n' and g using Eq. (11); actually we determine the three related parameters a, b, and C. This may be done by considering allowed

[9] D. M. Gruen, J. G. Conway, and R. D. McLaughlin, J. Chem. Phys. **25**, 1102 (1956).

[10] P. A. Sellers, S. M. Fried, R. E. Elson, and W. H. Zachariasen, J. Am. Chem. Soc. **76**, 5935 (1954).

transitions, e.g., the high-field line H_4 in Fig. 3, for which

$$\nu = w(M=-\tfrac{1}{2}, m_f=-2) - w(M=\tfrac{1}{2}, m_f=-1)$$
$$= -bH_4 - a[(1-2CH_4+C^2H_4^2)^{\frac{1}{2}} + (1-CH_4+C^2H_4^2)^{\frac{1}{2}}]. \quad (12)$$

This assumes that $a<0$ and $C>0$, but the same frequency (for the same sign of b) is obtained for $a>0$ and $C<0$ because the order of the states becomes changed about. However, a different frequency results for a, $C>0$ or a, $C<0$. We wish to point out that it is considerably simpler and less ambiguous to use the forbidden transitions to determine $|C|$ and $|a|$, since the frequency is independent of the sign choice and also b is not involved. From Eq. (11) we see that

$$\nu = 2|a|[1+|C|h_{12}+C^2h_{12}^2]^{\frac{1}{2}} = 2|a|[1+C^2h_{23}^2]^{\frac{1}{2}}$$
$$= 2|a|[1-|C|h_{34}+C^2h_{34}^2]^{\frac{1}{2}}, \quad (13)$$

from which we may directly determine $|C|$ and $|a|$ using the measured quantities ν, h_{12}, h_{23}, and h_{34}, without solving quadratic equations. For example, $|C|=h_{12}/(h_{23}^2-h_{12}^2)$, etc. Proceeding in this fashion we calculate from the data of Table I the values of $|C|$ and $|a|$ in Table II. There is a small consistent, angular variation of $|a|$ of about 0.1%, which may reflect a real anisotropy in the hfs A tensor. The average value is

$$|A|/h \equiv |a| = 1578.6 \pm 1.4 \text{ Mc/sec}, \quad (14a)$$

where the error represents deviations from isotropy rather than experimental error. From this value of $|a|$ we calculate $|a|/c = 0.05265 \pm 0.00005$ cm^{-1}.

Having so determined good values of $|a|$ and $|C|$, we substitute these into equations like Eq. (12) for various sign choices, and, using the measured values of ν, H_1, $H_2\cdots$ for the allowed transitions, we determine $|b|$ and also the sign of g_n' relative to g. The result is $|b|=1.2$ ± 0.2 (Mc/sec) (koe)$^{-1}$, and $g_n'/g<0$. The absolute or relative sign of $a=A/h$ is not determined. Since there is strong evidence from the shell model that the nuclear magnetic moment is positive, corresponding to $g_n'>0$ and $b<0$, we conclude that g is negative. From $|C|$ and the value of $g_n'=7.74\times10^{-4}$ as determined in ENDOR experiments described below, we calculate g from Eq. (11b). It also shows a slight consistent angular variation, perhaps representing a real anisotropy of the g tensor of about 0.2%. The average value in Table II is

$$g = -1.1423 \pm 0.0014. \quad (14b)$$

This value uniquely determines $\theta=40.9°$ in Eq. (7) and corresponds to a value of $V/\zeta \cong 1.004$ in Eq. (5). This value of θ inserted into Eq. (8) yields

$$A = -4.57 g_n \beta^2 \langle r^{-3} \rangle, \quad (14c)$$

showing that the sign of A should be negative. Note that the expressions in Eq. (8) and Eq. (14c) neglect any s-state contributions to the hyperfine splitting, since there is at present no reliable estimate of this effect for $5f$ configurations, although it is presumed to be of minor importance.

In an attempt to determine g_n' more precisely, an ENDOR experiment was performed by observing the change in the intensity of the H_1 line at high microwave power upon application of a second frequency ${}_1\nu_n$, ${}_2\nu_n\cdots$. At a microwave frequency $\nu \approx 9.44$ kMc/sec, $H_1 \approx 4.294$ koe, and $T \sim 1.6°$K, a small effect ($<1\%$) was observed at the frequencies $\nu_n \approx 580$ Mc/sec and $\nu_n \approx 656$ Mc/sec, which agree, respectively, with calculated values of ${}_6\nu_n$ and ${}_1\nu_n$ (Fig. 3) using the values of $|a|$, $|b|$, and $|C|$ previously determined and assuming $g_n'/g<0$. Similar results were obtained for the lines at H_2 and H_3, and although they confirm the relative sign determination, $g_n'/g<0$, these measurements do not provide data which yield a much more precise value of g_n' because none of the ENDOR frequencies observed formed a "lucky pair"[11]: From Eq. (11) it follows that if H is constant ${}_5\nu_n - {}_1\nu_n = 2|b|H$, so that the observation of this pair of frequencies will yield $|b|$ and hence $|g_n'|$ directly and independently of $|a|$, $|C|$, etc. Presumably the para-

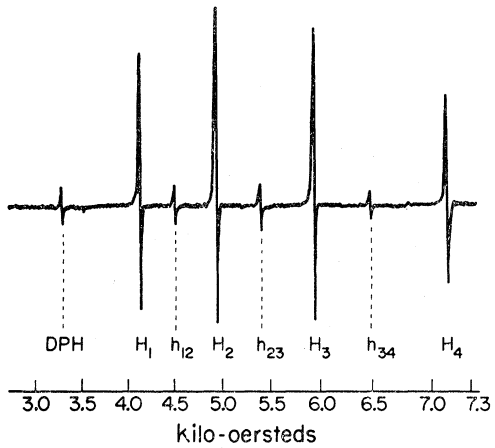

FIG. 5. Derivative of paramagnetic resonance absorption of $\approx 1\%$ tetravalent Pa^{231} in a single crystal of Cs_2ZrCl_6 at $\nu=9.168$ kMc/sec and $T=1.6°$K. The lines H_1, $H_2\cdots$ are M, $m \rightarrow M\pm1$, m transitions; the lines h_{12}, h_{23}, and h_{34} are M, $m \rightarrow M\pm1$, $m\mp1$ transitions. The DPH line is that of diphenyl-picryl-hydrazil.

TABLE I. Measured values of the paramagnetic resonance lines H_1, h_{12}, etc., for tetravalent Pa^{231} in Cs_2ZrCl_6 at $\nu=9.267$ kMc/sec and $T=1.6°$ K. The orientation refers to an arbitrary rotation of the crystal about the z'' axis of Fig. 4.

	Relative orientation			
Line	0° koe	30° koe	60° koe	90° koe
H_1	4.1740	4.1755	4.1765	4.1810
h_{12}	4.5520	4.5525	4.5545	4.5590
H_2	4.9910	4.9925	4.9950	5.0000
h_{23}	5.4500	5.4510	5.4545	5.4600
H_3	5.9840	5.9865	5.9905	5.9960
h_{34}	6.5250	6.5265	6.5320	6.5380
H_4	7.1520	7.1550	7.1625	7.1685

[11] J. Eisinger and G. Feher, Phys. Rev. **109**, 1172 (1958).

TABLE II. Values of $|C|$ and $|a|$ calculated from data of Table I using Eq. (13), and values of $|g|$ then calculated from Eq. (11b), using $g_n'=7.74\times10^{-4}$. The errors for the average values indicate the limits of anisotropy.

Relative orientation	$\|C\|$ in $(\text{koe})^{-1}$	$\|a\|$ in Mc/sec	g
0°	0.50684±0.00003	1577.27±0.01	−1.1432±0.00007
30°	0.50646±0.0002	1578.4 ±0.1	−1.1430±0.0005
60°	0.5057 ±0.0001	1579.3 ±0.1	−1.1421±0.0002
90°	0.5051 ±0.0003	1579.6 ±0.2	−1.1409±0.0007
Average	0.5060 ±0.0009	1578.6 ±1.4	−1.1423±0.0014

magnetic relaxation rates for this spin system are such that saturation of the allowed transitions does not produce a very large population difference between levels connected by "lucky pair" ENDOR frequencies. Then when the oscillating field at ν_n is applied, the populations cannot be changed sufficiently to allow for detection. Since it is known from dynamic nuclear orientation experiments[12] that saturation of the forbidden transitions is a much more effective way of producing large population differences between adjacent hfs states, we then performed an ENDOR experiment by observing the change in intensity of a partially saturated forbidden line, h_{23}, which had a signal to noise ratio of 100:1. A large effect ($\sim10\%$) was observed, as shown in Fig. 6, for $\nu_n=684.6$ Mc/sec and $\nu_n=696.2$ Mc/sec, corresponding, respectively, to ${}_1\nu_n$ and ${}_5\nu_n$. Another lucky pair, ${}_2\nu_n$ and ${}_4\nu_n$, was also observable, but the effect was smaller. The experiments were done by fixing the field at either the positive or negative peak of the derivative of the absorption curve and then recording the change as the General Radio oscillator frequency was slowly varied in the neighborhood of ${}_1\nu_n$ and ${}_5\nu_n$. The results of several runs are summarized in Table III. In order to eliminate the error introduced by the fact that the data are taken at either the low or the high side of the h_{23} line rather than at the center, we average the values of $({}_5\nu_n-{}_1\nu_n)/2H$ to obtain

$$|b|=1.083\pm0.01\ (\text{Mc/sec})\ (\text{koe})^{-1}, \qquad (15)$$

yielding $|g_n'|=7.74\times10^{-4}$ and $|\mu_n'|=I|g_n'|(1836)=2.13$ nuclear magnetons. Within the experimental error of $\approx1\%$, $|b|$ was found to be independent of crystal orientation in the H field. Similar ENDOR experiments on the h_{12} and h_{34} lines gave a value of $|b|$ in agreement with Eq. (15).

In adopting the spin Hamiltonian formalism, no allowance is made for the mixing of crystal quantum states due to the magnetic field or hyperfine interaction. Although these second-order effects are small, Baker and Bleaney[6] have pointed out that they may be comparable with or larger than the direct nuclear Zeeman interaction. In the present case, nonvanishing matrix elements of the form

$$2g_n\beta^2\langle r^{-3}\rangle[\langle\Gamma_7|(\mathbf{l}+2\mathbf{s})\cdot\mathbf{H}|\Gamma_i\rangle\langle\Gamma_i|\mathbf{N}\cdot\mathbf{I}|\Gamma_7\rangle+\langle\Gamma_7|\mathbf{N}\cdot\mathbf{I}|\Gamma_i\rangle\langle\Gamma_i|(\mathbf{l}+2\mathbf{s})\cdot\mathbf{H}|\Gamma_7\rangle] \qquad (16)$$

(where $|\Gamma_7\rangle$ refers to the ground-state doublet and $|\Gamma_i\rangle$ to the excited f^1 levels of the complex) produce isotropic energy shifts proportional to $\mathbf{H}\cdot\mathbf{I}$ in the Γ_7 states. These effects appear in the parameter g_n' in the spin Hamiltonian along with the true nuclear g factor. Since the terms in Eq. (16) are isotropic, they may be evaluated most conveniently by placing $H=H_z$, in which case the correction to the nuclear g factor becomes:

$$g_n'=g_n+0.0460\sum_i\frac{\langle\Gamma_7|l_z+2s_z|\Gamma_i\rangle\langle\Gamma_i|N_z|\Gamma_7\rangle}{E(\Gamma_i)-E(\Gamma_7)}, \qquad (17)$$

where $E(\Gamma_i)-E(\Gamma_7)$ are expressed in cm^{-1}, $g_n\beta^2\langle r^{-3}\rangle$ being evaluated by means of Eq. (14c). Although we shall postpone the details and discussion for a future publication, for purposes of the above correction we shall report the following conclusions obtained from a study of the near infrared spectrum of the $PaCl_4-Cs_2ZrCl_6$ system. A comparison of three observed absorption bands with the theoretical fit obtained using the values $\zeta=1490\ \text{cm}^{-1}$, $V=1496\ \text{cm}^{-1}$, $V'=2160\ \text{cm}^{-1}$ is shown in Fig. 2(d). These values were chosen so as to also give the observed g value for the Γ_7 level. Adopting these values, the summation in Eq. (17) gives

$$g_n'-g_n=0.6296\times10^{-4}, \qquad (18)$$

from which we find for the nuclear magnetic moment of Pa^{231}

$$\mu_n=Ig_n\times(1836)=1.96\ \text{nuclear magnetons}. \qquad (19)$$

Nearly the entire correction is due to the nearest lying Γ_8 level approximately 1900 cm^{-1} above the ground state. Although this level has not yet been detected optically, its existence is strongly indicated by the good fit for the higher levels.

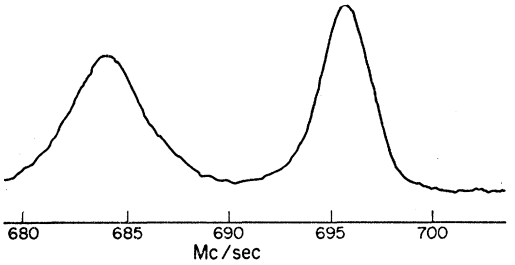

FIG. 6. Intensity of the h_{23} line of Fig. 5 as a function of the second frequency ν_n. The ENDOR "lines" at $\nu_n=684.6$ Mc/sec and $\nu_n=696.2$ Mc/sec correspond to the ${}_1\nu_n$ and ${}_5\nu_n$ transitions of Fig. 3.

[12] C. D. Jeffries, Phys. Rev. **117**, 1056 (1960).

TABLE III. Summary of ENDOR experiments on the h_{23} resonance line of tetravalent Pa^{231} in Cs_2ZrCl_6 at $\nu=9.168$ kMc/sec, $T=1.6°K$. The first column gives the relative orientation of the crystal about the z'' axis, Fig. 4. The second column gives the field value and indicates whether it was slightly above or below the line center. The third, fourth, and fifth columns give the average of the measured values, ${}_1\nu_n$, ${}_5\nu_n$ and $({}_5\nu_n-{}_1\nu_n)/2H$ for about 4 runs.

Relative orientation	$H\approx h_{23}$	${}_1\nu_n$ in Mc/sec	${}_5\nu_n$ in Mc/sec	$({}_5\nu_n-{}_1\nu_n)/2H$ in (Mc/sec) (koe)$^{-1}$
0°	5.408 koe (high side)	684.57±0.03	696.22±0.02	1.077±0.008
0°	5.3855 koe (low side)	684.25±0.07	695.98±0.01	1.090±0.002
45°	5.3895 koe (high side)[a]	684.69±0.05	696.31±0.01	1.078±0.01

[a] The center of the h_{23} resonance line has shifted due to the rotation of the crystal.

Substitution of our measured values of g_n and A into Eq. (14c) yields an "experimental" value of 5.53 atomic units for $\langle r^{-3}\rangle$. This value may be compared with 3.89 atomic units obtained from a SCF (without exchange) calculation for neutral uranium[13]; and 4.8 atomic units obtained for Np^{6+} using an approximate Thomas-Fermi potential.[4] Our value seems somewhat too large to be in really good agreement with the theoretical numbers although it is perhaps not unexpected in view of the approximations involved in obtaining both our value and the theoretical ones.

Since there was good reason to believe that the Pa^{4+} ion might have a small hfs interaction with the six Cl nearest neighbors and the eight Cs next nearest neighbors, etc., a low-frequency ENDOR experiment was performed by observing the change in the intensity of the microwave line at $H_1=4007\pm5$ oe while applying a second frequency ν_n'' in the range 350 kc/sec $<\nu_n''<50$ Mc/sec. An effect, shown in Fig. 7, was indeed observed centered about $\nu_n''=2.244\pm0.005$ Mc/sec, which we identify with the calculated Cs^{133} nuclear resonance frequency $\nu=2.238\pm0.003$ Mc/sec, in the H_1 field. A similar ENDOR pattern, centered about the Cs nuclear resonance frequency was observed

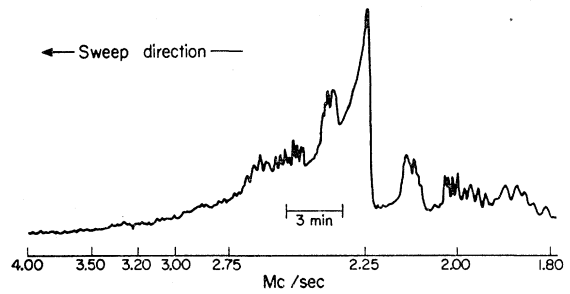

FIG. 7. Intensity of the H_1 line of Fig. 5 as a function of the second frequency ν_n''. These low-frequency ENDOR lines reveal a hfs interaction of Pa^{4+} with Cs^{133} in $Cs_2(Pa,Zr)Cl_6$.

[13] J. C. Hubbs, R. Marrus, W. A. Nierenberg, and J. L. Worcester, Phys. Rev. **109**, 390 (1958).

for the microwave line at $H_3=5.814$ koe. No other lines were seen although a nonreproducible line near 32 Mc/sec sometimes appeared. The spectrum at H_1 was recorded for two angular positions of the crystal in the magnetic field differing by 30°. The pattern changed but remained centered at the same central frequency. At least 40 lines were observed and appeared to fall into 8 groups symmetrically paired about the center.

The central ENDOR line appeared to have a much longer characteristic decay time than the symmetrically paired lines, and we associate it with Cs nuclei so far removed from a Pa^{4+} site that there is negligible hfs interaction and a correspondingly longer nuclear relaxation time.[14] We must add to Eq. (6) the term

$$-g_n''\beta\mathbf{H}\cdot\mathbf{I}'', \tag{20}$$

where the double primed quantities refer to Cs^{133}. The other lines we associate with the eight Cs nuclei at the corners of the cube, Fig. 1, which may have in addition to Eq. (20) a hfs interaction with the central Pa^{4+} ion of the form

$$A''I_{zi}''S_{zi}+B''(I_{xi}''S_{xi}+I_{yi}''S_{yi}), \tag{21}$$

where the directions $z_1, z_2\cdots$ represent the four body-diagonal directions. If this term is small compared to Eq. (20), then the low-frequency ENDOR transitions corresponding to $M, m, m''\rightarrow M, m, m''\pm1$ occur at the frequencies

$$\nu_n''(\theta_i)\approx\left|-\frac{g_n''\beta H}{h}\pm\frac{1}{2h}[A''^2\cos^2\theta_i+B''^2\sin^2\theta_i]^{\frac{1}{2}}\right|, \tag{22}$$

where θ_i is the angle between z_i and H. The $\pm$ sign arises because of $M=\pm\frac{1}{2}$. The ENDOR spectrum thus should consist of a pair of lines centered approximately about $\nu_n=g_n''\beta H/h$ for each of the four z_i directions. These lines could be further split by Cs^{133} ($I=\frac{7}{2}$) interactions with the electric field gradient, resulting in the groups shown in Fig. 7. We have not attempted to analyze the spectrum in detail, but from the maximum and minimum spacings of the groups for various crystal orientations we estimate that A''/h and B''/h have the order of magnitude of 0.2 to 0.8 Mc/sec.

The assumed form of Eq. (21) has a theoretical justification: One may use the Γ_7 ground-state functions

[14] This central line is basically distinct from the usual ENDOR lines and is due to the fact that our observation of the electron resonance is a few oersteds below or above the peak; this induces forbidden transitions which simultaneously flip electron and nuclear spins and the distant Cs nuclei become dynamically polarized. An analysis [O. S. Leifson and C. D. Jeffries (to be published)] of the rate equations for the whole system yields the transient behavior of Fig. 7, the decay time of central line being roughly T_1 for the distant Cs nuclei. The phenomenon is similar to that of R. W. Terhune, J. Lambe, G. Makhov, and L. G. Cross, Phys. Rev. Letters **4**, 234 (1960).

[Eq. (2) with $\theta=40.9°$] to show that the angular distribution of the electron charge density is proportional to $x^2y^2z^2$ plus other terms like $z^2(x^4+y^4)$, etc. This distribution points along the body diagonals of the Cs cube and gives rise to the $Pa^{4+}-Cs^{133}$ hfs observed in Fig. 7. We note in passing that the resolution is very high, splitting (presumably quadrupolar) as small as 10 kc/sec being resolved in some cases.

ACKNOWLEDGMENTS

We wish to acknowledge with much thanks the stimulating advice and help of Professor B. B. Cunningham on the preparation of Pa^{4+} in a solid matrix; the assistance of Professor Roy Anderson on the design and construction of the paramagnetic resonance apparatus; and the helpful collaboration of Dr. Ru-tao Kyi on preliminary resonance experiments.

PHYSICAL REVIEW VOLUME 121, NUMBER 6 MARCH 15, 1961

Electrical Resistivity of Lanthanum, Praseodymium, Neodymium, and Samarium*

J. K. Alstad, R. V. Colvin,† S. Legvold, and F. H. Spedding
Institute for Atomic Research and Department of Physics, Iowa State University, Ames, Iowa
(Received November 9, 1960)

The electrical resistivities of polycrystalline samples of La, Pr, Nd, and Sm are reported in the temperature range 1.3°K to 300°K. La exhibits a superconducting transition at 5.8°K. The curve for Pr has slope changes at 61°K and 95°K. The Nd curve shows small jumps at 5°K and 20°K. Sm shows slope changes at 14°K and 106°K.

MEASUREMENTS on the resistivities of the light rare earths were reported by James *et al.*[1] in 1952. Improved techniques for producing metals of higher purity have led to the measurements on La, Pr, Nd, and Sm reported here. Some improvement has also been made in the experimental procedure and apparatus. The present work is an extension of the results of Colvin *et al.*[2] and Curry *et al.*[3] on the electrical resistivity of the other polycrystalline rare-earth metals, and completes the work.

The samples were prepared from arc-melted buttons of the metals. These were turned to cylinders approximately $\frac{3}{16}$ inch in diameter by 2 inches long. The results of analyses for impurities are shown in Table I. The resistivities of the samples were measured in the cryo-

Table I. Analysis (in %).

Element	Impurities (determined from spectrographic and vacuum fusion analysis)
Lanthanum	Ce≤0.03, Pr≤0.03, Nd≤0.02, Ca≤0.01, Fe<0.15, Si<0.01, Mg<0.01, Ta<0.2. Cu, Ni,Sm, trace present.
Praseodymium	Nd≤0.02, Ce≤0.1, La≤0.005, Ca≤0.1, Fe≤0.02, Mg<0.01, Si<0.025, Ta≤0.2, Cr<0.01, O≤0.094, H≤0.0005, N≤0.0920. Ca, Cu, Mn, Ni, Ti, Y, trace present.
Neodymium	Sm≤0.06, Pr≤0.08, Ca<0.05, Mg<0.01, Fe≤0.005, Si<0.025, Ta<0.1, Cr<0.01 0≤0.035. B, Mn, Ni, trace present.
Samarium	Ca<0.03, Fe<0.005, Mg<0.01, Si<0.01, Cu≤0.05, Gd≤0.02, Nd≤0.02, Eu≤0.005.

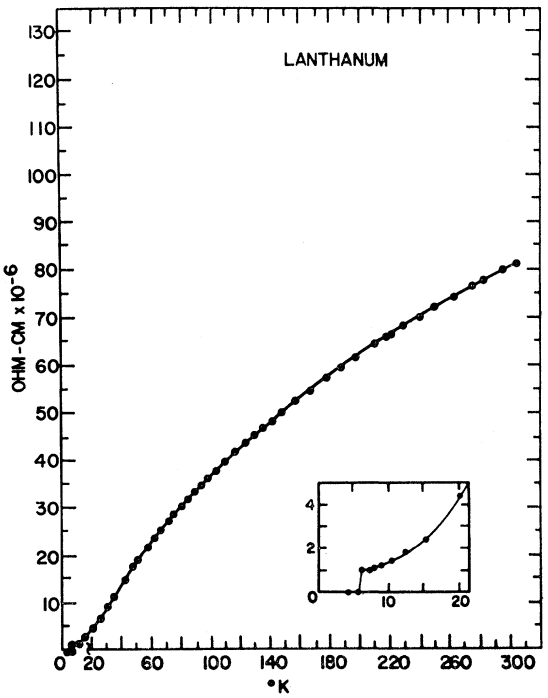

Fig. 1. The electrical resistivity of La vs temperature.

* Contribution No. 951. Work was performed in the Ames Laboratory of the U. S. Atomic Energy Commission.

† Now at the Edgar C. Bain Laboratory of the U. S. Steel Corporation, Monroeville, Pennsylvania.

[1] N. R. James, S. Legvold, and F. H. Spedding, Phys. Rev. **88**, 1092 (1952).

[2] R. V. Colvin, S. Legvold, and F. H. Spedding, Phys. Rev. **120**, 741 (1960).

[3] M. A. Curry, S. Legvold, and F. H. Spedding, Phys. Rev. **117**, 953 (1960).